International Journal of Heat and Mass Transfer 52 (2009) 2466–2470

Contents lists available at ScienceDirect

International Journal of Heat and Mass Transfer

journal homepage: www.elsevier.com/locate/ijhmt

Onset of convection in a horizontal porous layer driven by catalytic surface reaction on the lower wall

Adrian Postelnicu

Department of Thermal Engineering and Fluid Mechanics, Transilvania University of Brasov, Bd Eroilor 29, 500036 Brasov, Romania

ARTICLE INFO

Article history:
Received 27 September 2007
Received in revised form 29 December 2008
Available online 5 March 2009

Keywords:
Porous layer
Onset of convection
Catalytic surface reaction

ABSTRACT

The onset of convection in a horizontal layer filled with a fluid-saturated porous medium is studied in this paper. On the lower wall there is an exothermic surface reaction, described by the Arrhenius kinetics, while the upper wall is subjected to uniform temperature and concentration. The problem, cast in dimensionless form, is governed by three dimensionless parameters pertaining to the exothermic reaction and the Lewis number. Once the basic state is solved, a linearized stability analysis is then performed and the resulting eigenvalue problem is solved using a conventional shooting method. One determines numerically the critical Rayleigh and wave numbers at the onset of convection, for various values of the problem parameters.

1. Introduction

Literature concerning convective flow in porous media is abundant. Much of the recent work in this area and more specifically to convection in fluid-saturated porous layers may be found in the recent books [1–9].

However, recent years revealed an increased interest about fluid and thermal systems where chemical reactions take place. These chemical reactions may undergo throughout the volume of (porous) region which is analyzed or along interfaces/boundaries of this region. Real-world applications include chemical engineering systems, contaminant transport in groundwater systems, or geothermal processes. The catalytic systems are modeled usually by including the description of the reaction kinetics of the catalytic process and the transport of momentum, heat, and mass coupled to this process. Concerning the transport phenomena, access to the catalyst is determined by the transport of mass and energy in a reactor. In heterogeneous catalysis, the access to the catalyst is maximized through the use of porous structures. Examples of catalytic surface reactions are methane/ammonia and propane oxidation over platinum, see for instance [10,11].

Many papers focusing on chemically reacting flows were devoted in the past to the situation where the reaction occurs in a spatially manner, see the references contained in [12]. But our interest in the present context is related to the chemical reactions which take place along interfaces/boundaries of the flow region.

In clear fluids a number of papers dealing with the effects of catalytic chemical reactions on external convective processes appeared in the last years. In [13] the free-convection boundary-layer flow at a three-dimensional stagnation point of attachment on a curved surface, due to an exothermic catalytic chemical reaction on that surface is considered. It is assumed that the flow is driven purely by heat supplied to the surrounding fluid by an exothermic catalytic chemical reaction on the surface and this reaction can be modeled using single, first-order Arrhenius kinetics. Other two important papers focusing on free-convection stagnation point driven by the same mechanism of catalytic surface reaction are [14,15], while [16,17] are studies in the same area, involving flows along vertical surfaces in viscous fluids.

Models for convective flows on reactive surfaces in porous media have been proposed for external flows by Merkin and Mahmood [18], Mahmood and Merkin [19], Minto et al. [20]. The study by Merkin and Mahmood [18] was extended by Postelnicu [21] for porous media saturated with non-Newtonian fluids. In both [18,21] bifurcation diagrams were presented for various combinations of the problem parameters and hysteresis bifurcation curves were identified, whenever they exist.

We consider in this paper the situation when the convective flow in the porous layer is driven by an exothermic catalytic reaction taking place on the lower surface whereby a reactive species P reacts to form an inert product Q. On the upper surface usual boundary conditions of uniform temperature and concentration are imposed.

It seems, at the author's best knowledge, that this kind of boundary conditions have been not taken into account till now in the analysis of the onset of convection in horizontal fluid-saturated porous layers. Thus, the aim of the present paper is to find how the critical Rayleigh number is modified by these boundary conditions.

E-mail address: adip@unitbv.ro

0017-9310/$ - see front matter © 2009 Elsevier Ltd. All rights reserved.
doi:10.1016/j.ijheatmasstransfer.2009.01.021

Nomenclature

A, B	dimensionless parameters, defined in (13)
C	concentration
D	thermal diffusion of the porous medium
h	depth of the horizontal layer
E	activation energy
k	wave number
k_0	rate constant
k_m	thermal conductivity of the porous medium
k_T	thermal conductivity of the surface
K	permeability
Le	Lewis number
Q	heat of reaction
R^*	universal gas constant
R	Rayleigh number
u, v	components of the Darcian velocity in the x- and y-direction
T	temperature
t	time
x, y	co-ordinates along the porous layer and normal to it, respectively

Greek symbols

β	coefficient of thermal expansion
ε	activation energy parameter
φ	dimensionless concentration
κ	thermal diffusivity of the porous medium
θ	dimensionless temperature
ρ	density
ψ	stream function

Subscripts

b	basic state
c	critical value
r	reference conditions

2. Analyis

We consider a horizontal layer, see Fig. 1, of depth h, filled with a fluid-saturated porous medium. The upper wall is subjected to uniform temperature and concentration, while on the lower wall there is an exothermic surface reaction, whereby reactant P is converted to an inert product Q via the following first-order non-isothermal reaction

$$P \rightarrow Q + \text{heat}, \ \text{rate} = k_0 C \exp\left(-\frac{E}{R^* T}\right) \tag{1}$$

known as the Arrhenius kinetics. Here E is the activation energy, R^* is the universal gas constant, k_0 is the rate constant, T is the temperature and C is the concentration of reactant P within the convective fluid. This reaction scheme is a realistic one and has been used in the past in modeling of combustion processes, and also for reactive processes in porous media [18–21]. As noted in [18,19], the surface reaction releases heat, which produces a convective flow close to the surface and, in turn, fresh reactant will replace that used up in the reaction. In this way, an interaction will occur between the convective flow, heat transfer and mass transport of the reactant.

Using usual notations, the governing equations which describe the problem at hand are mass conservation, Darcy's law, equation of energy and that of concentration

$$\frac{\partial \bar{u}}{\partial \bar{x}} + \frac{\partial \bar{v}}{\partial \bar{y}} = 0 \tag{2}$$

$$\bar{u} = -\frac{K}{\mu}\frac{\partial \bar{p}}{\partial \bar{x}}, \bar{v} = -\frac{K}{\mu}\frac{\partial \bar{p}}{\partial \bar{y}} + \frac{\rho g \beta K}{\mu}(T - T_r) \tag{3}$$

$$\frac{\partial T}{\partial \bar{t}} + \bar{u}\frac{\partial T}{\partial \bar{x}} + \bar{v}\frac{\partial T}{\partial \bar{y}} = \kappa\left(\frac{\partial^2 T}{\partial \bar{x}^2} + \frac{\partial^2 T}{\partial \bar{y}^2}\right) \tag{4}$$

$$\frac{\partial C}{\partial \bar{t}} + \bar{u}\frac{\partial C}{\partial \bar{x}} + \bar{v}\frac{\partial C}{\partial \bar{y}} = D\left(\frac{\partial^2 C}{\partial \bar{x}^2} + \frac{\partial^2 C}{\partial \bar{y}^2}\right) \tag{5}$$

where T_r is a reference temperature and over-bars refer to dimensional quantities. The $\bar{x}$ and $\bar{y}$ axes are taken along the porous layer and normal to it, respectively, and the lower wall is located at $\bar{y} = 0$. We point out that in writing Eq. (3), the Boussinesq approximation was invoked and differences in reactant concentration (which may induce buoyancy forces) are assumed to be small. The Darcy's model is justifiable when the heat of reaction is small or moderate. Otherwise, when the heat of reaction is large, non-Darcy models must be used, see also [12,22].

The thermal boundary conditions on the lower wall are

$$k_T \frac{\partial T}{\partial \bar{y}} = -Q k_0 C \exp\left(-\frac{E}{R^* T}\right), D\frac{\partial C}{\partial \bar{y}} = k_0 C \exp\left(-\frac{E}{R^* T}\right) \tag{6}$$

where k_T is the thermal conductivity of the surface, Q is the heat of reaction, which is taken as positive, meaning that heat is taken from the surface into the surrounding fluid-porous medium by conduction. Eliminating the pressure, using the streamfunction ψ and introducing the dimensionless quantities

$$x = \frac{\bar{x}}{h}, y = \frac{\bar{y}}{h}, t = \frac{h^2}{\kappa}\bar{t}, u = \frac{\kappa}{h}\bar{u}, v = \frac{\kappa}{h}\bar{v}, \theta = \frac{E}{R^* T_r^2}(T - T_r), \varphi = \frac{C}{C_r} \tag{7}$$

Eqs. (1)–(4) become

$$\frac{\partial^2 \psi}{\partial x^2} + \frac{\partial^2 \psi}{\partial y^2} = R\frac{\partial \theta}{\partial x} \tag{8}$$

$$\frac{\partial \theta}{\partial t} + u\frac{\partial \theta}{\partial x} + v\frac{\partial \theta}{\partial y} = \frac{\partial^2 \theta}{\partial x^2} + \frac{\partial^2 \theta}{\partial y^2} \tag{9}$$

$$\frac{\partial \varphi}{\partial t} + u\frac{\partial \varphi}{\partial x} + v\frac{\partial \varphi}{\partial y} = \frac{1}{Le}\left(\frac{\partial^2 \varphi}{\partial x^2} + \frac{\partial^2 \varphi}{\partial y^2}\right) \tag{10}$$

where $Le = \kappa/D$ is the Lewis number and R is the Rayleigh number defined as

$$R = \frac{\rho g \beta K h}{\mu \kappa} \cdot \frac{R^* T_r^2}{E} \tag{11}$$

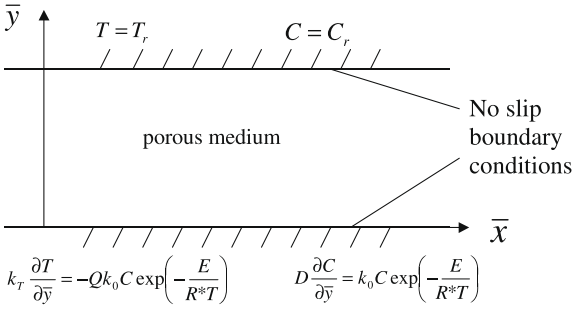

Fig. 1. Geometry of the problem.

The boundary conditions are

$$\psi = 0, \text{ on both } y = 0 \text{ and } y = 1 \tag{12a}$$

$$\frac{\partial \theta}{\partial y} = -A\varphi \exp\left(\frac{\theta}{1+\varepsilon\theta}\right), \frac{\partial \varphi}{\partial y} = B\varphi \exp\left(\frac{\theta}{1+\varepsilon\theta}\right), \text{ on } y = 0 \tag{12b}$$

$$\theta = 0, \varphi = 1, \text{ on } y = 1 \tag{12c}$$

where two dimensionless parameters A and B are introduced

$$A = \frac{Qk_0C_0h}{k}\cdot\frac{E}{R^*T_r^2}, B = \frac{k_0h}{D}, \varepsilon = \frac{R^*T_r}{E} \tag{13}$$

and ε is the activation energy parameter.

2.1. Basic state

The basic state is motionless $u_b = v_b = \psi_b = 0$ and is characterized by the linear temperature and concentrations profiles

$$\theta_b = ay + b, \varphi_b = cy + d \tag{14}$$

where the constants a, b, c, and d are obtained by enforcing the boundary conditions (12). The following algebraic system is obtained

$$a = -Ad\exp\left(\frac{b}{1+\varepsilon b}\right), c = Bd\exp\left(\frac{b}{1+\varepsilon b}\right),$$

$$a + b = 0, c + d = 1 \tag{15}$$

By combining these equations, we obtain the transcendental equation in a

$$a + (A + Ba)\exp\left(-\frac{a}{1-\varepsilon a}\right) = 0 \tag{16}$$

where three parameters are involved: A, B and ε.

2.2. Stability analysis

Expressing

$$\psi = \Psi, \theta = \theta_b + \Theta = ay + b + \Theta, \varphi = \varphi_b + \Phi = cy + d + \Phi \tag{17}$$

where Ψ, Θ and Φ are perturbed quantities, $|\Psi| \ll 1$, $|\Theta \ll 1$ and $|\Theta| \ll 1$, the linearized stability problem is governed by the equations

$$\frac{\partial^2\Psi}{\partial x^2} + \frac{\partial^2\Psi}{\partial y^2} = R\frac{\partial\Theta}{\partial x} \tag{18}$$

$$\frac{\partial\Theta}{\partial t} + a\frac{\partial\Psi}{\partial x} = \frac{\partial^2\Theta}{\partial x^2} + \frac{\partial^2\Theta}{\partial y^2} \tag{19}$$

$$\frac{\partial\Phi}{\partial t} + c\frac{\partial\Psi}{\partial x} = \frac{\partial^2\Phi}{\partial x^2} + \frac{\partial^2\Phi}{\partial y^2} \tag{20}$$

subject to the boundary conditions

$$\Psi = \Theta = 0, \text{ on } y = 0 \text{ and } y = 1 \tag{21a}$$

$$\frac{d\Theta}{dy} = -A\Phi\exp\left(\frac{\Theta}{1+\varepsilon\Theta}\right), \frac{d\Phi}{dy} = B\Phi\exp\left(\frac{\Theta}{1+\varepsilon\Theta}\right), \text{ on } y = 0 \tag{21b}$$

$$\Theta = \Phi = 0, \text{ on } y = 1 \tag{21c}$$

Now, taking into account that Θ and Φ are small quantities, the boundary conditions (21b) can be linearized to give

$$\frac{d\Theta}{dy} = -A\Phi, \frac{d\Phi}{dy} = B\Phi, \text{ on } y = 0 \tag{21d}$$

Looking for the solutions in the form

$$\Psi = e^{\lambda t}f(y)\sin kx, \Theta = e^{\lambda t}g(y)\cos kx, \Phi = e^{\lambda t}h(y)\cos kx \tag{22}$$

Eqs. (18)–(20) become

$$f'' - k^2 f + kRg = 0 \tag{23}$$

$$g'' - (k^2 + \lambda)g + akf = 0 \tag{24}$$

$$h'' - (k^2 + \lambda)h + ckf = 0 \tag{25}$$

which must be solved along the boundary conditions

$$f(0) = 0, g'(0) = -Ah(0), h'(0) = Bh(0) \tag{26a}$$

$$f(1) = 0, g(1) = 0, h(1) = 0 \tag{26b}$$

The problem formulated in (23)-(26) is an eigenvalue problem, which must be solved for the Rayleigh number.

It can be shown that the principle of exchange of stability holds, so we can take $\lambda = 0$ in the previous equations. We mention that a problem where the frequency (λ in our case) is real, so that the marginal stability occurs when $\lambda = 0$, is said to obey the principle of exchange of stability.

However, since there are no analytical solution of this eigenvalue problem, it will be solved numerically, by minimizing the Rayleigh number over the wave number. The corresponding values of the wavenumber and Rayleigh number are termed critical.

3. Numerical results

Eq. (16) was solved using an usual algebraic root solver, based on interpolation and bisection methods. Solutions for the unknown a are presented in Table 1, where various values between 0 and 5 were assigned for A and B, while the activation energy parameter ε was set to 0, 0.15 and 0.5, see for instance [18,22]. The eigenvalue problem (23)–(26) was solved using a traditional shooting method. A number of trials were performed in order to obtain grid-independence results.

Before proceed further, it is important to ascertain the accuracy of our eigenvalue solver. With this aim, we used alternatively the routine dissolve from MAPLE 8. In Table 2 there is shown a comparison between the results obtained by the shooting method and those provided by MAPLE. One remarks that the agreement is very good, so that we are confident in our method.

We present further, in Table 3, critical values of Rayleigh number as a function of A, B, ε and Le. We mention that in our numerical simulations the Lewis number was taken as: 0.1, 1, 10 and 100.

- Inspection of Table 3 reveals that the effect of ε is to slowly increase the critical Rayleigh number, at given A and B, for any Lewis number.
- Another important observation is concerning the combinations of A and B which significantly increase the critical Rayleigh number. They are those with B smaller than A: we point out the maximum value of R_c which is 878.561, attained for $Le = 100$, $B = 0.5$, $A = 5$ and $\varepsilon = 0.5$.

Table 1
Solutions of Eq. (16).

A	B	ε	a	A	B	ε	a
0.5	0.5	0	−0.43609	0.5	1	0	−0.28544
0.5	0.5	0.15	−0.42770	0.5	1	0.15	−0.28382
0.5	0.5	0.5	−0.41322	0.5	1	0.5	−0.28061
0.5	5	0	−0.08447	1	0.5	0	−1.28976
0.5	5	0.15	−0.08446	1	0.5	0.15	−1.13888
0.5	5	0.5	−0.08443	1	0.5	0.5	−0.98295
1	1	0	−0.65905	1	5	0	−0.17115
1	1	0.15	−0.64244	1	5	0.15	−0.17105
1	1	0.5	−0.61554	1	5	0.5	−0.17081
5	1	0	4.96536	5	5	0	−0.92663
5	1	0.15	−4.70158	5	5	0.15	−0.91807
5	1	0.5	−3.95265	5	5	0.5	−0.90305

Table 2
Comparisons of critical wavenumber and Rayleigh number for $\varepsilon = 0.5$ and several values of A, B and Le.

A	B	Le	(k_c, R_c)	
			Shooting	Maple
1	1	0.1	2.336, 43.931	2.351, 44.534
1	0.5	0.1	2.326, 27.379	2.342, 27.755
0.5	0.5	1	2.326, 69.359	2.491, 70.048

Table 3
Critical Rayleigh number as a function of A, B, ε and Le.

A	B	ε	R_c			
			$Le = 0.1$	$Le = 1$	$Le = 10$	$Le = 100$
0.5	0.5	0	61.714	65.722	95.844	155.892
0.5	0.5	0.15	62.924	67.010	97.723	158.947
0.5	0.5	0.5	65.130	69.359	101.149	164.520
0.5	1	0	94.737	104.656	171.674	249.877
0.5	1	0.15	95.278	105.253	172.654	251.303
0.5	1	0.5	96.369	106.459	174.631	254.182
0.5	5	0	324.941	406.310	741.858	878.088
0.5	5	0.15	324.995	406.377	741.982	878.234
0.5	5	0.5	325.116	406.529	742.258	878.561
1	0.5	0	20.866	22.145	32.406	52.709
1	0.5	0.15	23.631	25.079	36.700	59.692
1	0.5	0.5	27.379	29.058	42.521	69.161
1	1	0	41.032	45.328	74.354	108.224
1	1	0.15	42.092	46.499	76.276	111.022
1	1	0.5	43.931	48.531	79.608	115.873
1	5	0	160.376	200.536	366.147	433.384
1	5	0.15	160.478	200.663	366.380	433.659
1	5	0.5	160.697	200.937	366.880	434.252
5	1	0	26.366	27.014	32.770	43.101
5	1	0.15	27.846	28.530	34.608	45.520
5	1	0.5	33.122	33.937	41.166	54.146
5	5	0	29.622	37.040	67.629	80.048
5	5	0.15	29.899	37.386	68.260	80.795
5	5	0.5	30.396	38.007	69.396	82.139

In Fig. 2 there is depicted the variation of the critical wave number with B, for $A = 0.5$ and $\varepsilon = 0.5$. It is seen that, at given Lewis number, the critical wave-number increases with B, while increase of the Lewis number leads to an increase of k_c.

Critical Rayleigh number vs B is shown in Fig. 3, when $A = 0.5$ and $\varepsilon = 0.5$. The critical Rayleigh number increases with B, almost linearly for small Lewis number. On the other hand, we remark the usual increase of R_c with Le, a value near 240 being reached by the critical Rayleigh number for $B = 1$, when $Le = 100$.

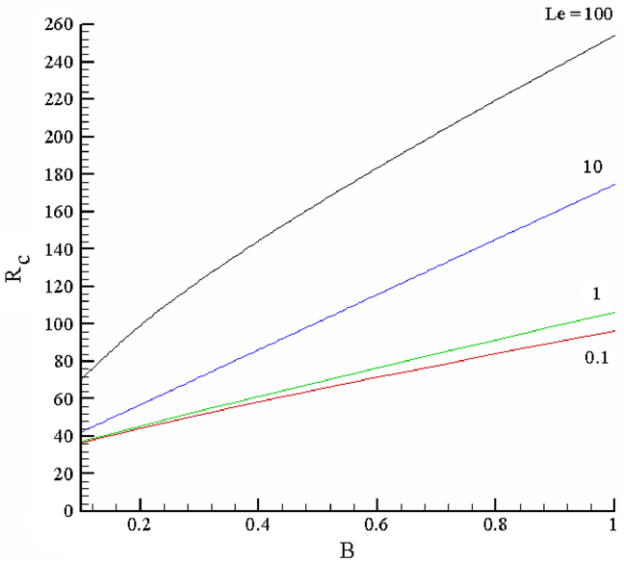

Fig. 3. Variation of the critical Rayleigh number with B, for $A = 0.5$ and $\varepsilon = 0.5$.

Fig. 4 depicts the critical Rayleigh number as a function of A, for $B = 5$ and $\varepsilon = 0$. Now the monotonicity of R_c with A is opposite as compared with Fig. 2. But the above quoted remark, on the increase of R_c with Le holds, as expected.

Sharp variation of k_c as a function of the Lewis number is observed in Fig. 5 ($A = 1$, $B = 5$ and $\varepsilon = 0.5$), till Le reaches approximately 15, then the curve flattens at a value of five of the critical wave number. A somewhat similar situation occurs with the critical Rayleigh number, for Le less than 25 and further, after this value, R_c increases slightly till about 440, when $Le = 100$, see Fig. 6.

4. Conclusion

In this paper the onset of convection in a horizontal layer filled with a fluid-saturated porous medium is investigated numerically. On the lower wall there is an exothermic surface reaction, de-

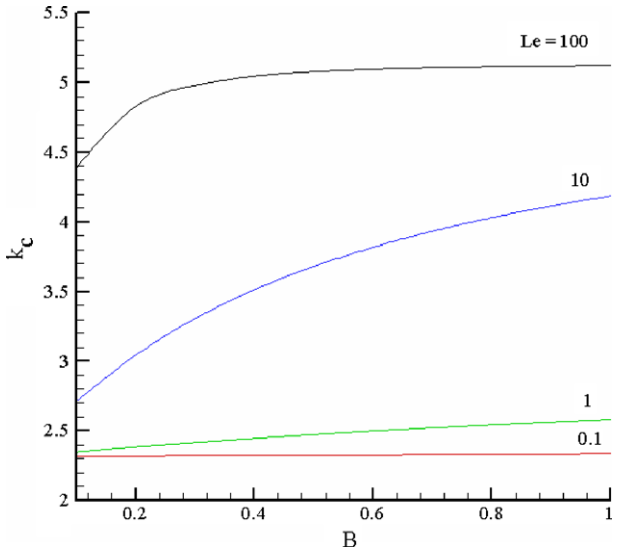

Fig. 2. Variation of the critical wave number with B, for $A = 0.5$ and $\varepsilon = 0.5$.

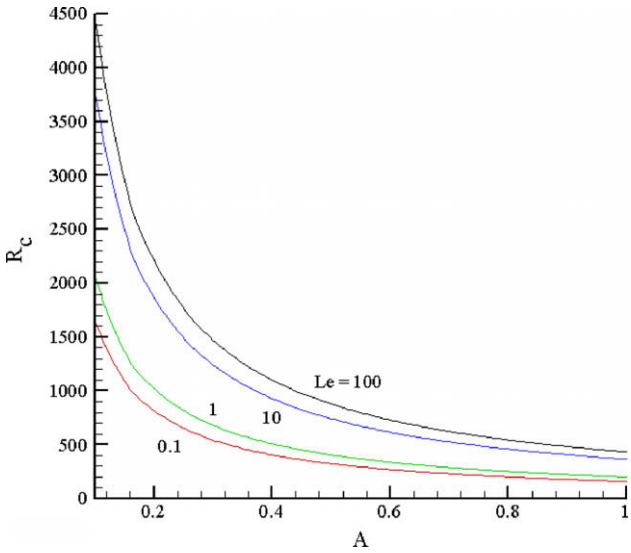

Fig. 4. Critical Rayleigh number as a function of A, for $B = 5$ and $\varepsilon = 0$.

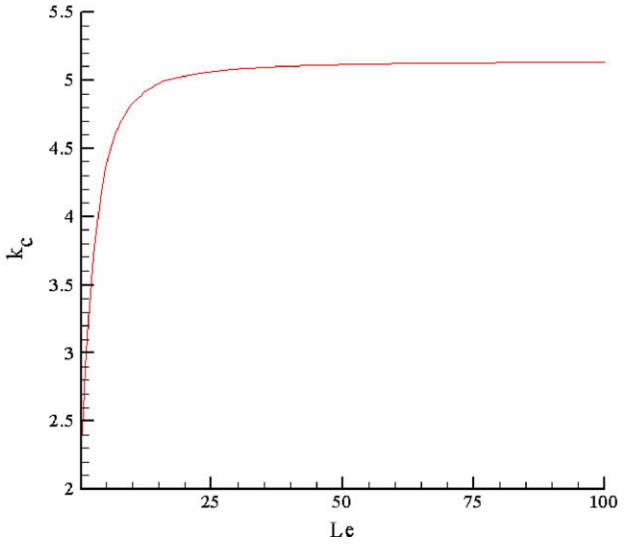

Fig. 5. Values of the critical wave number vs Lewis number, for $A = 1$, $B = 5$ and $\varepsilon = 0.5$.

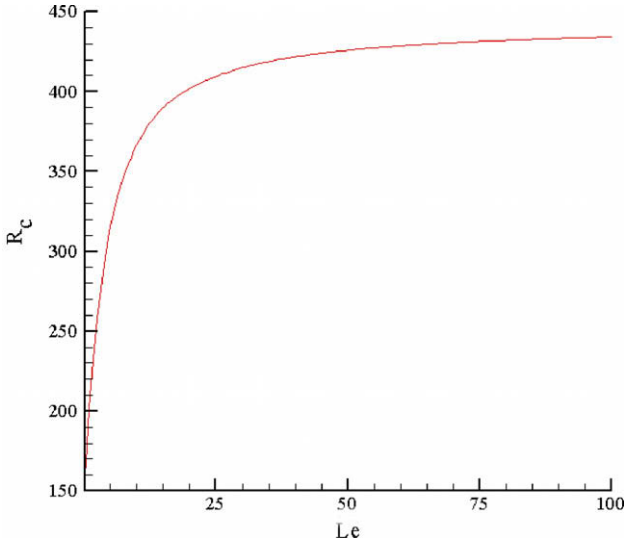

Fig. 6. Values of the critical Rayleigh number vs Lewis number, for $A = 1$, $B = 5$ and $\varepsilon = 0.5$.

scribed by the Arrhenius kinetics, while the upper wall is subjected to uniform temperature and concentration. The basic state is motionless, but with linear temperature and concentration profiles. We found that in comparison with the classical Darcy–Benard problem, of porous layers heated from below and cooled from above, there are significant differences, due to the parameters involved in the basic state, which are present also in the (linearized) stability equations.

We mention to this end that a preliminary version of this study was presented in [23].

References

[1] A. Bejan, I. Dincer, S. Lorente, A.F. Miguel, A.H. Reis, Porous and complex flow structures in modern technologies, Springer, New York, 2004.
[2] D.B. Ingham, I. Pop (Eds.), Transport Phenomena in Porous Media I, Pergamon, Oxford, 1998.
[3] D.B. Ingham, I. Pop (Eds.), Transport Phenomena in Porous Media II, Pergamon, Oxford, 2002.
[4] D.B. Ingham, I. Pop (Eds.), Transport Phenomena in Porous Media III, Elsevier, Oxford, 2005.
[5] D.B. Ingham, A. Bejan, E. Mamut, I. Pop (Eds.), Emerging Technologies and Techniques in Porous Media, Kluwer, Dordrecht, 2004.
[6] I. Pop, D.B. Ingham, Convective Heat Transfer: Mathematical and Computational Modelling of Viscous Fluids and Porous Media, Pergamon, Oxford, 2001.
[7] D.A. Nield, A. Bejan, Convection in Porous Media, second edition., Springer, New York, 1999.
[8] K. Vafai (Ed.), Handbook of Porous Media, second ed., Taylor & Francis, New York, 2005.
[9] D.A.S. Rees, The stability of Darcy–Benard convection, in: K. Vafai (Ed.), Handbook of Porous Media, Marcel Dekker, 2000, pp. 521–558.
[10] X. Song, W.R. Williams, L.D. Schmidt, R. Aris, Steady state and oscillations in homogeneous-heterogeneous reaction systems, Chem. Eng. Sci. 46 (1991) 1203–1215.
[11] W.R. Williams, J. Zhao, L.D. Schmidt, Ignition and extinction of surface and homogeneous oxidation of NH_3 and CH_4, AIChe J. 37 (1991) 641–649.
[12] H.D. Nguyen, S. Paik, R. Douglas, I. Pop, Unsteady non-Darcy reaction-driven flow from an anisotropic cylinder in porous media, Chemical Eng. Sci. 51 (1996) 4963–4977.
[13] D.B. Ingham, S.D. Harris, I. Pop, Free-convection boundary layers at a three-dimensional stagnation point driven by exothermic surface reaction, Hybrid Methods Eng. 1 (1999) 401–417.
[14] M.A. Chaudhary, J. Merkin, Free convection stagnation point boundary layers driven by catalytic surface reactions: I. The steady states, J. Eng. Math. 28 (1994) 145–171.
[15] M.A. Chaudhary, J. Merkin, Free convection stagnation point boundary layers driven by catalytic surface reactions: II. Times to ignition, J. Eng. Math. 30 (1996) 403–415.
[16] J. Merkin, M.A. Chaudhary, Free convection boundary layers on vertical surfaces driven by an exothermic surface reaction, Quart. J. Appl. Math. 47 (1994) 405–428.
[17] M.A. Chaudhary, A. Liffan, J. Merkin, Free convection boundary layers driven by exothermic surface reactions: critical ambient temperature, Math. Eng. Ind. 5 (1995) 129–145.
[18] J. Merkin, T. Mahmood, Convective flows on reactive surfaces in porous media, Transport Porous Media 33 (1998) 279–293.
[19] T. Mahmood, J. Merkin, The convective boundary-layer flow on a reacting surface in a porous medium, Transport Porous Media 32 (1999) 285–298.
[20] B.J. Minto, D.B. Ingham, I. Pop, Free convection driven by an exothermic on a vertical surface embedded in porous media, Int. J. Heat Mass Transfer 41 (1998) 11–23.
[21] A. Postelnicu, Free convection near a stagnation point of a cylindrical body in a porous medium saturated with a non-Newtonian fluid, in: A.H. Reis, A.F. Miguel (Eds.), International Conference on Applications of Porous Media (ICPAM 2004), Evora, Portugal, May 24–27, 2004, pp. 231–236.
[22] K. Vafai, C. Desai, S.C. Chen, An investigation of heat transfer process in a chemically reacting packed bed, Num. Heat Transfer A 24 (1993) 127–142.
[23] A. Postelnicu, Onset of convection in a horizontal porous layer driven by catalytic surface reaction, Paper Number 5, Proceedings of ICAPM, Third International Conference on Applications of Porous Media, May 29–June 3, 2006, Marrakech, Morocco.